TU Delft

Delft University of Technology

Morphological Adaptation of River Channels to Vegetation Establishment
A Laboratory Study

Vargas-Luna, Andrés; Duró, Gonzalo; Crosato, Alessandra; Uijttewaal, Wim

DOI
10.1029/2018JF004878

Publication date
2019

Document Version
Final published version

Published in
Journal of Geophysical Research: Earth Surface

Citation (APA)
Vargas-Luna, A., Duró, G., Crosato, A., & Uijttewaal, W. (2019). Morphological Adaptation of River Channels to Vegetation Establishment: A Laboratory Study. *Journal of Geophysical Research: Earth Surface*, *124*(7), 1981-1995. https://doi.org/10.1029/2018JF004878

Important note
To cite this publication, please use the final published version (if applicable).
Please check the document version above.

Copyright
Other than for strictly personal use, it is not permitted to download, forward or distribute the text or part of it, without the consent of the author(s) and/or copyright holder(s), unless the work is under an open content license such as Creative Commons.

Takedown policy
Please contact us and provide details if you believe this document breaches copyrights.
We will remove access to the work immediately and investigate your claim.

This work is downloaded from Delft University of Technology.
For technical reasons the number of authors shown on this cover page is limited to a maximum of 10.

JGR Earth Surface

RESEARCH ARTICLE
10.1029/2018JF004878

Morphological Adaptation of River Channels to Vegetation Establishment: A Laboratory Study

Andrés Vargas-Luna[1], Gonzalo Duró[2], Alessandra Crosato[2,3], and Wim Uijttewaal[2]

[1]Department of Civil Engineering, Pontificia Universidad Javeriana, Bogotá, Colombia, [2]Faculty of Civil Engineering and Geosciences, Delft University of Technology, Delft, The Netherlands, [3]Department of Water Science and Engineering, IHE Delft Institute for Water Education, Delft, The Netherlands

Key Points:
- The effects of vegetation establishment depend on the colonized area within the river
- Bar morphology is affected by vegetation establishment on riverbanks and on emerging sediment deposits
- Vegetation establishment on emerging bar surfaces enhances river meandering or anabranching

Correspondence to:
A. Vargas-Luna,
avargasl@javeriana.edu.co

Citation:
Vargas-Luna, A., Duró, G., Crosato, A., & Uijttewaal, W. (2019). Morphological adaptation of river channels to vegetation establishment: A laboratory study. *Journal of Geophysical Research: Earth Surface*, *124*, 1981–1995. https://doi.org/10.1029/2018JF004878

Received 13 SEP 2018
Accepted 30 JUN 2019
Accepted article online 10 JUL 2019
Published online 26 JUL 2019

©2019. American Geophysical Union. All Rights Reserved.

Abstract While the scientific community has long recognized that alluvial rivers are the product of interactions between flowing water and bed material transport, it is increasingly evident that vegetation mediates these interactions and influences the stream channel characteristics. In a novel set of mobile bed laboratory experiments with variable discharge, we demonstrate that vegetation colonization affects bank erosion rates, channel shape, channel sinuosity, and bar pattern. Our analyses compared the morphological evolution of channels with initially steady bars considering the following three scenarios: (1) channel without vegetation, (2) channel with vegetation added to the floodplains, and (3) channel with vegetation added to both the floodplains and the bar surfaces that emerge at low flows. Absence of vegetation produced the widest and shallowest channel with the lowest sinuosity. Floodplain vegetation in the second scenario reduced bank erosion and resulted in a deeper and more sinuous channel with shorter bars. In the third scenario, vegetation establishment on emerging bar surfaces intensified erosion on the opposing bank, enlarging the amplitude of bends. Enhanced sedimentation on vegetated bar areas increased both bar elevation and bar length compared to the second scenario. The results show that the colonization of bar surfaces by plants creates the conditions for new floodplain and island formation, fostering channel meandering and anabranching. Finally, our experiments emphasize the role of alternating high and low flows on the morphological development of streams mediated by vegetation.

1. Introduction

River morphology results from the interaction between flowing water, sediment transport, and vegetation (Bertagni et al., 2018; Corenblit et al., 2009; Gurnell et al., 2012; Paola, 2011). Different river configurations might be expected depending on vegetation establishment, which is in turn influenced by river processes. Plants colonizing floodplains and bar surfaces emerging during low flows act as ecosystem engineers (Gurnell, 2014; Jones et al., 1994; van de Koppel et al., 2001). By increasing the hydraulic resistance (Tsujimoto, 1999; Zong & Nepf, 2011), vegetation reduces the local flow velocity (Vargas-Luna et al., 2015), enhancing fine sediment deposition (Cotton et al., 2006; Meier et al., 2013; Nepf, 2012; Sand-Jensen & Mebus, 1996; Wu & He, 2009). In turn, the local settling of fine sediment coming from upstream and organic matter from the plants, rich in nutrients, controls plant survival and growth and promotes the establishment of new vegetation communities (succession). The settling of fine sediment also promotes soil consolidation processes, further increasing resistance against erosion of the vegetated surfaces (Allmendinger et al., 2005; van de Koppel et al., 2001). Colonization of sediment deposits, such as bars, by pioneer plants is therefore the first step toward the accretion of riverbanks and the transformation of these deposits into new islands or floodplains (Asahi et al., 2013; Bertoldi et al., 2014; Wintenberger et al., 2015). As a result, the riverbed and width change together with the river planform (Millar, 2000, 2005; Murray & Paola, 2003; Perucca et al., 2007; Eaton et al., 2010; Crosato & Samir Saleh, 2011; Gleason, 2015; Iwasaki et al., 2016).

Since the pioneering work carried out by Hickin (1984), several studies have examined the effects of vegetation establishment on rivers from field observations (e.g., Serlet et al., 2018 [alternate bars]; Gran et al., 2015 [braided rivers], Bywater-Reyes et al., 2018 [sinuous channels]). The presence of vegetation favors the stability of recently formed deposits and banks by deflecting the flow and increasing soil strength due to the mechanical reinforcement derived from root networks (Bywater-Reyes et al., 2018; Pollen & Simon, 2005; Pollen-Bankhead & Simon, 2010; Polvi et al., 2014). Vegetation furthermore decreases erosion by

covering and, therefore, protecting the bare soil and reduces the pore water pressure by lowering the soil moisture content via interception and evapotranspiration (e.g., Terwilliger, 1990). However, it is important to point out that the presence of vegetation may also decrease bank stability because of increased infiltration rates during rainfall events (Collison & Anderson, 1996; Simon & Collison, 2002) and the additional weight on banks (Abernethy & Rutherfurd, 2000).

Vegetation tends to grow on steady or slowly migrating bars, because bar movement tends to rework the soil, eradicating plants. Vegetation on floodplains reduces bank erosion and the channel width-to-depth ratio, decreasing the amount of bars forming in unvegetated channels (Jang & Shimizu, 2005, 2007). Therefore, to understand how vegetation changes river morphology, it is crucial to reveal how the establishment of vegetation on bars and floodplains affects the morphological evolution of river systems. This is also essential for assessing the potential impact of human activities, such as floodplain vegetation management, upstream dam construction, water withdrawal, and the construction of drainage systems that alter the surface and subsurface flow regimes of a river and affect riparian vegetation (e.g., Egger et al., 2015; van Ruijven & Berendse, 2005).

The morphology and rigidity of plants influence the flow turbulence, alter the flow resistance of vegetated beds, and considerably affect banks. Recent research provides some understanding of the interaction between flow dynamics and plants [see Green, 2005; Nikora, 2010; Folkard, 2011; Nepf, 2012; Marjoribanks et al., 2014, for a review]. However, the results of these studies are only applicable to a few plant species (or plant surrogates in most cases) under controlled laboratory conditions, which might differ from those observed in nature (Vargas-Luna et al., 2016). One of the critical obstacles to applying these results in the field is the complex distribution of riparian vegetation along river corridors. Riparian vegetation cover typically combines different species, densities, and developmental stages, which are influenced by the local geology as well as by the hydrologic regime and climate of the area.

Several mathematical and numerical models simulate the effects of plants on river hydrodynamics, sediment, and morphodynamic processes, notwithstanding some important limitations, such as treating plants as rigid cylinders (see Vargas-Luna, Crosato, & Uijttewaal, 2015, Vargas-Luna, 2016, for a review). A few 2-D models can reproduce river width variations treating bank erosion and accretion separately. However, in these models the representation of river bank accretion is still highly simplified (Asahi et al., 2013; Bertoldi et al., 2014; Bywater-Reyes et al., 2018; Jang & Shimizu, 2005, 2007; Kang et al., 2018).

Laboratory experiments that investigate the geomorphic effects of vegetation are less common. Still, researchers have shown how plants increase the local soil strength, stabilize the floodplain surface, and deflect the flow toward the center of the main channel, resulting in reduced braiding indices of the alluvial channel (e.g., Bertoldi et al., 2015; Braudrick et al., 2009; Gran & Paola, 2001; Tal & Paola, 2007; Tal & Paola, 2010). Rominger et al. (2010) described secondary flow alterations and increased bank erosion on the opposing bank due to the presence of plants. A recent flume investigation with real plants focused on the description of the topographic adjustments of a vegetated bed to different sediment supply conditions (Diehl et al., 2017), stressing the relevance of clarifying the morphological evolution of river bars with vegetation. Most of these experiments faced difficulties in measuring bed elevation changes and flow properties, restricting the quantitative interpretation and the upscaling of the observed responses relative to natural scales of rivers.

The vegetation colonization process varies in nature due to the interactions between vegetation dynamics and climate. In arid and cold climates, colonization by vegetation is relatively slow and occurs mainly during low-flow periods, with subsequent high-flow periods potentially eradicating the new fragile plants (Bertoldi et al., 2014). In these environments, vegetation is more likely to establish itself on floodplains only. In tropical and humid climates, instead, vegetation proliferates and is more likely to establish itself also on areas of the riverbed that emerge during low flows, namely bars (Bertoldi et al., 2014; Perucca et al., 2007). However, the effects of vegetation establishment on emergent bar surfaces also depend on river size. Quantifying these effects on river morphology is therefore complicated, because if the stream power of the river is large enough to eradicate young pioneer vegetation with sufficiently high frequency, vegetation might not be able to colonize bar tops even in tropical humid climates (Bankhead et al., 2017; Bywater-Reyes et al., 2015; Edmaier et al., 2011, 2015; Perona & Crouzy, 2018). Based on the above considerations, three different vegetation configurations might be encountered in natural channels: (1) no vegetation, (2) floodplain vegetation, and (3) vegetation on both floodplains and bar surfaces.

Climate change is likely to affect river morphology by altering the flow and sediment regimes (e.g., Lotsari et al., 2015; Mueller & Pitlick, 2013) and riparian vegetation (Perry et al., 2015). For instance, climate changes affecting the intensity of extreme events (droughts or floods) can cause abrupt alterations of the sediment transport rates and plant establishment (e.g., Asselman, 1995). As a consequence, during the last several decades, an increased frequency of climate-related vegetation mortality events has been observed, for instance, in forest ecosystems (Allen et al., 2010).

Our experimental investigation studies the role of vegetation establishment on the evolution of riverbed topography and planform style, analyzing the interaction between vegetation, riverbed, and bank dynamics. The experiments quantitatively examine the development of initially straight channels shaped by variable flow over a sandy bed that is subsequently perturbed by vegetation colonization. As accretion processes in rivers commonly start with colonization by vegetation of the emerging parts of sediment deposits, such as bars, during low flows, the experiments include: a mobile-bed channel with erodible banks bounded by a floodplain, variable discharge, quasi-stable alternate bars, and vegetation.

Two types of vegetation establishment are studied; the first considers vegetation colonization on river floodplains only, while the second includes vegetation colonization on the floodplains and on the bar surfaces that emerge during low flows. These two cases are compared to a reference case without vegetation, but with very similar initial conditions, allowing quantification of the effects of the selected vegetation establishment types on the morphological development of the modeled stream.

The experiments describe systems in which plants are not easily eradicated and are inspired by the Lunterse beek, a well-monitored, small stream located in the Netherlands in which the conditions considered here were observed (see Vargas-Luna et al., 2018, for a complete description). However, the results of our experiments are not intended to be scaled with this or any other specific river.

The results show how channel characteristics and planform style respond to vegetation establishment on floodplains and emerging bars during low flows. In particular, the work quantitatively assesses the change of bar characteristics in terms of bar mode, wavelength, and amplitude following vegetation establishment.

2. Materials and Methods

2.1. Bars

Bars can be subdivided into two types: local and periodic. Alternate bars belong to the latter. Periodic bars form in alluvial channels due to morphodynamic instability (Engelund, 1970). There are two types of periodic bars: free and hybrid (Duró et al., 2016). The former are typically migrating whereas the latter are steady, fixed by the presence of some geometrical discontinuity of the channel which forces the flow pattern, such as a groyne, a bridge pile, or a local width variation. The bar mode is a parameter commonly used to identify the type of bars present in a channel: a mode of 1 corresponds with alternate bars, a mode of 2 corresponds with central bars, and modes larger than 2 correspond with multiple bars (Engelund, 1970). Considering bars as double harmonic waves of the channel bed with longitudinal and transverse wavelengths, the bar mode is theoretically represented as the integer of the ratio between two times the channel width and the transverse bar wavelength. For hybrid bars, that is, those bars that develop due to morphodynamic instability, but are fixed by forcing (Duró et al., 2016), the theoretical bar mode can be calculated using the formula derived by Crosato and Mosselman (2009), which is applicable only for width-to-depth ratios smaller than 100. If the flow can be assumed uniform, the formula becomes

$$m^2 = 0.17g\frac{(b-3)}{\sqrt{\Delta D_{50}}}\frac{B^3 i}{CQ} \tag{1}$$

in which m is the bar mode (-), g is the acceleration due to gravity (m/s^2), B is the channel width (m), i is the longitudinal bed slope (-), Δ is the submerged relative sediment density $(\rho_s\text{-}\rho_w)/\rho_s$=1.65 (-), where ρ_s and ρ_w are the sediment and water densities (kg/m^3), respectively, D_{50} is the median sediment size (m), C is the flow resistance in the form of the Chézy coefficient (m$^{1/2}$/s), Q is the flow discharge (m^3/s), and b is the degree of nonlinearity of the sediment transport formula as a function of flow velocity, written as

$$q_s = Mu^b \tag{2}$$

where q_s is the volumetric sediment transport rate per unit width (m^2/s), M is a coefficient, and u is the flow velocity (m/s). Crosato and Mosselman (2009) suggest imposing $b = 4$ for sand-bed rivers and $b = 10$ for

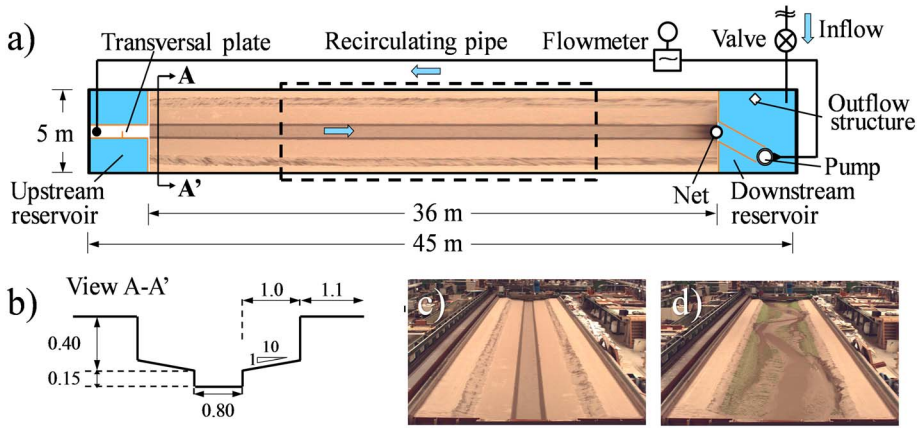

Figure 1. Experimental setup of the mobile bed flume: (a) planview, (b) initial configuration of cross-section A-A′ (vertically distorted 1V:2H), and initial (c) and final (d) planforms obtained for Scenario 3. The dashed square indicates the area used to report the reach-averaged characteristics of the channel. All dimensions in meters.

gravel-bed rivers. Due to the small size of the channel, the well-graded sand used in the experiments is expected to have mobility that is typical of gravel-bed rivers, that is, close to the conditions of initiation of motion (e.g., Le et al., 2018). For this reason, we considered both values of b to provide a theoretical range for the bar mode.

In our experiments, bars are preferably alternate and steady, because low bar dynamics is necessary for vegetation establishment. For this reason, the experimental setup needs a transverse plate at the upstream boundary, fixing the bar position, that is, producing hybrid bars (Crosato et al., 2012; Duró et al., 2016). The bar wavelength should allow observing several bars. This is obtained by selecting a discharge regime using the theory developed by Struiksma et al. (1985), described also in Crosato and Mosselman (2009). The conditions for alternate bar formation are described by equation (1) imposing mode $m = 1$. Considering that slope, width and the bed roughness are a result of the morphological adaptation of the system and cannot be imposed; determining the discharge regime requires a trial and error procedure (several preliminary experimental tests).

2.2. Experimental Setup

The experimental stream table was built in the Environmental Fluid Mechanics Laboratory of Delft University of Technology. It was 5 m wide and 45 m long but due to the inlet and outlet structures, the effective length became 36 m (Figure 1a). The facility was equipped with a reservoir located at the downstream end to control the downstream water levels during the experiments. From this reservoir, water and sediment were recirculated. A special sieve was designed and placed in the outlet structure to collect sediment samples and to dissipate excess energy of the incoming water (Figure 1a). The inlet structure included a 0.40-m-long transverse plate (half of the initial channel width) used as an upstream forcing with the aim to quickly obtain a regular, repeatable sequence of hybrid alternate bars, avoiding bar migration in the downstream part of the stream table (Crosato et al., 2012; Figure 1a).

A compound channel composed of a 0.80-m-wide and 0.15-m-deep channel, 1-m-wide floodplains, and 1.1-m-wide high terraces on both sides was excavated in the sediment at the start of every experiment (Figure 1b). The initial planform of one of the experiments is depicted in Figure 1c.

The sand used in the experiments had a median diameter, D_{50}, of 0.001 m and was selected based on experimental work carried out by Byishimo (2014) and Vargas-Luna et al. (2019). This previous research was focused on studying the effects of sediment properties and discharge variability on channel-width changes and was vital to select the sediment used in these experiments. Figure 2a shows the grain-size distribution of this material, which had a sorting index, I, of 2.26 given as

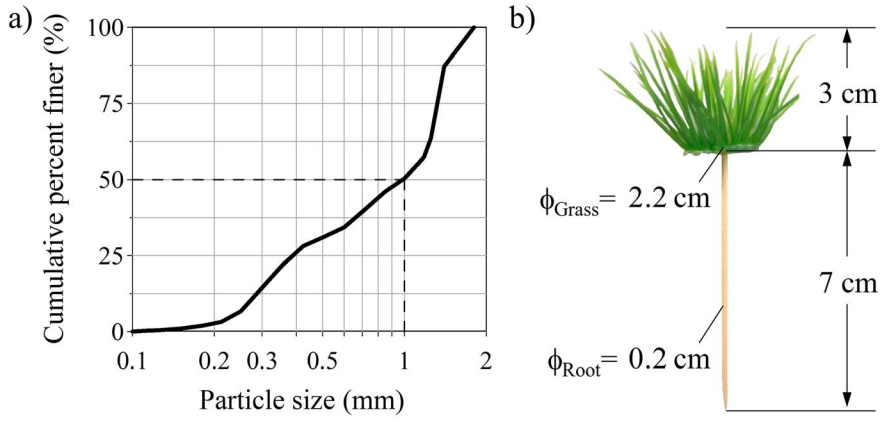

Figure 2. Materials used. (a) Grain size distribution of the sediment and (b) plants. ϕ_{Grass} and ϕ_{Root} correspond to the diameters of each element of plastic grass and its root, respectively.

$$I = 0.5\left(\frac{D_{84}}{D_{50}} + \frac{D_{50}}{D_{16}}\right) \tag{3}$$

where D_x is the diameter of the grain size exceeding x percentage of the material (Figure 2a).

Plastic plants of a grassy type were used in the experiments to represent the vegetation on the floodplains and the plants colonizing the emerging bar deposits. Velocity measurements were carried out by collecting high-quality photos from the ceiling of the laboratory to later apply the Particle Tracking Velocimetry methodology. The vegetation type, density, and placement were determined during preliminary experimental activities (Vargas-Luna, Crosato, & Uijttewaal, 2015,Vargas-Luna et al., 2015). From the results of testing different types and densities of vegetation (real, leafy plastic, grass-type plastic, and wooden cylinders), it was found that for the scale of the stream table, the grass-type plastic vegetation, provided with sticks mimicking roots, better reproduced the effects of the riparian vegetation found in small streams, such as reduction of bank erosion and deflection of the main flow velocity. An example of the plant units (root and foliage) used in these experiments is shown in Figure 2b. The medium plant density (112 plants per square meter) was selected among the three densities considered in the preliminary tests for the plastic grass (Vargas-Luna, Crosato, & Uijttewaal, 2015,Vargas-Luna, Crosato, Collot, & Uijttewaal, 2015). Wooden sticks were used as roots considering that they were found to be effective in reinforcing and protecting bare sediment banks and deposits from erosion in a way comparable to real roots (e.g., Vargas-Luna, 2016). Plants were manually inserted in the sand with a staggered pattern at the selected density over the area of interest following a light pattern projected on the sand surface. This vegetation configuration exhibits significant resistance for the flow intensity of our experimental stream. Similar characteristics were observed in the Lunterse beek in the Netherlands (e.g., Vargas-Luna et al., 2018).

2.3. Experimental Procedure

Prior to vegetation addition, each scenario started from the straight, excavated, compound channel of Figure 1 (first stage), which gradually changed in shape due to erosion and deposition processes. During the second stage, two different vegetation colonization scenarios were applied. The experiments also included a scenario without vegetation, for comparison.

Several preliminary tests were carried out to select the flow regime, based on its capability of producing the desired size of alternate bars in the channel. The chosen regime is a sequence of low and high discharges of 22 and 45 L/s, having a duration of 9 and 2 hr, respectively. This corresponds to having low flow for 82% of the time and high flow for the remaining 18%. To comply with the different flow rates and minimize backwater effects, a difference of 0.05 m in the water level of the downstream reservoir was imposed between low and high flow conditions. To guarantee sediment mobility during the experiment and to avoid significant bar pattern changes between the two discharges, the high-to-low flow ratio defined for this setup is not as high as that observed in real rivers (the low- and high-flow depths are approximately 50 and 75% of the thalweg bankfull depth, respectively, at the end of the first stage of each experiment, when the channel morphology has stabilized). The low and high flows selected for the experiments provided substantial differences in water

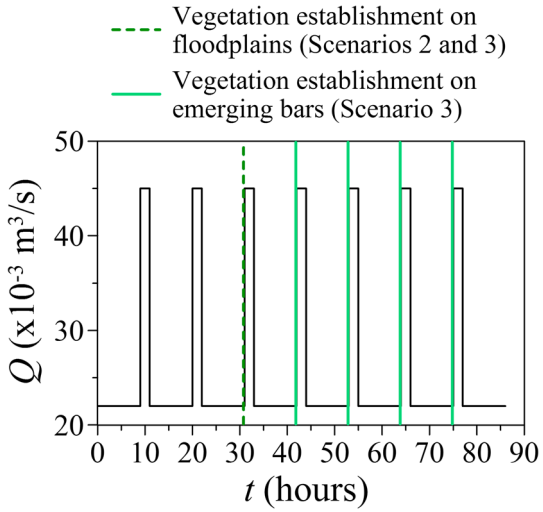

Figure 3. Discharge, *Q*, as a function of time indicating the scenarios and the vegetation establishment moments.

depth, allowing emergence of bar topography and opportunities for vegetation colonization. The preliminary experiments allowed us to determine the duration of each experimental stage: 31 hr for the first stage, a time long enough for hybrid alternate bar formation, and 55 hr for the second stage. This resulted in a total duration of 86 hr for each scenario (Figure 3).

After the initial bed conditioning phase (first stage), three scenarios were investigated: (1) an alluvial river channel without vegetation, (2) a river channel with vegetation on the floodplains, and (3) a river channel with vegetation on floodplains and on the bar surfaces emerging during low-flow stages. In the first scenario, the experiment continued with the same sequence of low and high discharges with no vegetation added. In the second scenario, plastic plants were put on the floodplains after the first 31 hr. In the third scenario, plants were also put on the floodplains after 31 hr, but then more plants at the same density were placed on bar surfaces that emerged during low flows. Uprooted plants from collapsed banks were not replaced, but if a vegetated area was entirely covered by transported sediment, more vegetation was added on the top at the same density. This procedure was repeated at each subsequent hydrograph cycle, simulating plant colonization and establishment on emerging bars during low flow. The experiments were terminated when one bank of the laterally migrating channel reached the end of the floodplain (after 86 hr).

2.4. Measurements

The bed surface was scanned at the end of each day to measure the bed topography evolution using a FARO Focus 3-D laser scanner, allowing for accurate measurements with an error range of ±0.002 m. More specifications about this equipment can be found online (http://www.faro.com/). The obtained point clouds were postprocessed using the Cloud Compare software (http://www.cloudcompare.org). A series of high-frequency high-resolution photos of floating particles were taken hourly from the ceiling of the laboratory to infer the surface flow velocity field in localized areas of the channel.

Flow velocity patterns were later reconstructed by using the time-resolved digital Particle Tracking Velocimetry tool for Matlab, developed by Brevis et al. (2011); (http://ptvlab.blogspot.com). This technique was selected based on preliminary studies, which demonstrated that for the range of water depths present in these experiments, the immersion of any element in the water to measure vertical flow velocities (e.g., an Acoustic Doppler Velocimeter) creates considerable local scour, altering the channel bed. Oblique high-resolution photos of the entire stream table were taken at 5-min intervals to record the width and the planform evolution of the channel. Corrections were applied to these photos to reduce the distortion due to the angle of capture by using the ShiftN software (http://www.shiftn.de/). The corrected photos were used to evaluate the channel planform evolution during the experiment. A net placed at the exit of the stream table in the reservoir was used to collect the particles released upstream for flow velocity measurements and the uprooted plastic plants transported by the flow during the experiment.

The flow discharge was measured at the inlet of the stream table by installing an acoustic flow meter in the recirculating pipe, and sediment samples were taken hourly at the outlet of this conduit using a sieve. The collected sediment samples were dried and weighed to estimate the sediment transport rates. Hourly water level profiles were measured with a point gauge installed on the carriage of the stream table. The longitudinal bed slope and the channel sinuosity were derived at the start and the end of each scenario from the elevation and position of the thalweg. All channel characteristics that were derived from the measured data refer to the central 20 m of the 36 m stream table, avoiding the areas that were affected by the boundaries (Figure 1). However, the scans of bed topography shown in the results represent a 33 m extent. The following bar characteristics were measured at the start and the end of each experiment: bar length, bar amplitude, and bar mode; the last parameter is described in the following section.

2.5. Scaling Considerations

Even if our experiments were not meant to be a scale reproduction of any existing river, scale considerations are important for understanding the results. For instance, sand-bed rivers are characterized by higher

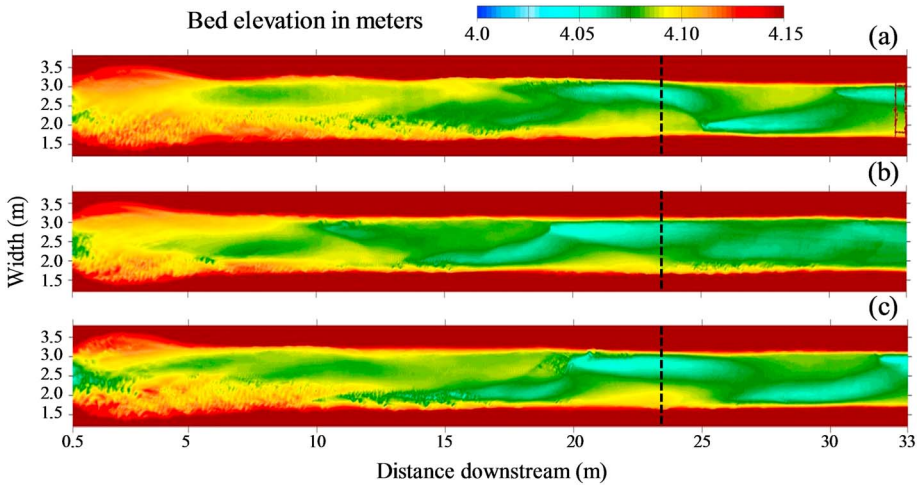

Figure 4. Measured bed elevation and planview of the channel after 31 hr for (a) Scenario 1, (b) Scenario 2, and (c) Scenario 3. Indicated cross sections are shown in Figure 5. Flow from left to right.

sediment mobility than gravel-bed rivers in which the conditions are close to the threshold for sediment motion (e.g., El Kadi Abderrazzak et al., 2014; Kleinhans et al., 2014). Sediment mobility is thus important for the interpretation of the observed morphodynamic processes at the scale or real rivers. Mobility depends on sediment diameter and density, flow velocity, and bed roughness, which in turn depend on channel bed topography and width, presence of vegetation, and bar characteristics (e.g., Van Rijn, 1993). In mobile bed experiments sediment mobility can be expected to vary with time. As an example, Figures 1c and 1d show the initial and final channel configuration of Scenario 3. Due to different vegetation configurations, in our experiments sediment mobility also depends on the particular vegetation scenario.

In general, the use of sand does not assure that our experimental scenarios represent the morphodynamic processes of sand-bed rivers, considering that upscaling of previous laboratory results has rather indicated that the sediment mobility obtained in laboratory streams with sandy beds is often closer to that of gravel-bed rivers (e.g., Le et al., 2018). The Shields (1936) parameter, θ_x, is commonly used to quantify sediment mobility, which for our analysis was computed at the start and the end of each scenario, from the values of the measured variables, as

$$\theta_x = \frac{u^2}{C^2 \Delta D_x} \tag{4}$$

where u is the flow velocity (m/s); and D_x is the sediment size (m) corresponding to the x percentile of the sediment distribution.

River channels are characterized also by two-dimensional morphodynamic processes leading to specific types of bed topography. Upscaling the 2-D morphodynamic behavior of our experiments is equivalent to reproducing the same bar typology (Kleinhans et al., 2014; section 2.1). The parameters that govern the bar characteristics are included in equation (1), which was derived from Struiksma et al.'s (1985) theory. This means that the experiments represent the 2-D morphodynamic behavior of river channels with hybrid bars having the same mode.

The upscaling of plants from the laboratory scale to the real-river scale is an unsolved problem. For this reason, the model grass was not meant to represent any particular prototype but rather to facilitate a general investigation of the effects of vegetation.

3. Results

The experimental results of the three scenarios can be compared to one another only if the starting conditions are the same or very similar. The similarity in the starting conditions (i.e., at the time of vegetation placement at 31 hr) is shown in Figures 4 and 5 that depict the bed elevation and cross sections at a selected

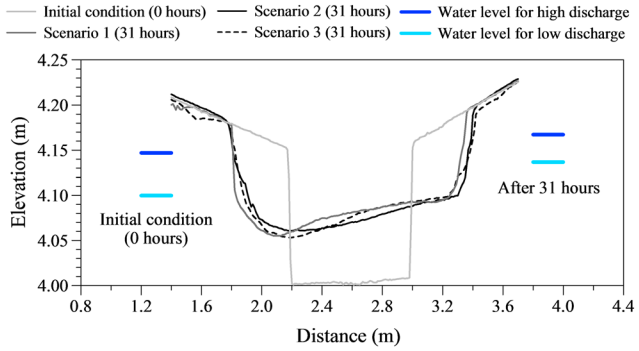

Figure 5. Cross-section comparison between the initial condition and bar development after 31 hr, the starting time for the considered scenarios. Location of the cross sections shown in Figure 4.

location and in Table 1 that lists the reach-scale characteristics of the three channels after 31 hr (prior to vegetation addition). The results of previous theoretical and numerical investigations (Duró et al., 2016; Struiksma et al., 1985) indicate that alternate bars develop at the same location if the flow and sediment conditions, as well as forcing, are the same. Our results show, however, that some small differences are present which could be the result of slight deviations in the experimental operations, in particular near the upstream boundary where some small sediment deposit could slightly deviate the water flow.

Figure 6 depicts the temporal evolution of the channel characteristics in the three scenarios starting from the conditions that were present after 31 hr (Figures 4 and 5 and Table 1). The wetted channel width (Figure 6a) corresponds to the averaged value of the free-surface width calculated by means of imagery analysis. As expected, width varies as a function of discharge. Scenario 1 (without plants) shows a similar widening rate during the entire experiment, whereas widening is moderately reduced in Scenarios 2 and 3 after the establishment of vegetation on floodplains. The final averaged width is reduced by approximately 10% in the scenarios with vegetation.

Figure 6b shows that the water depth in the vegetated cases is slightly larger compared to the nonvegetated case. This is due to the smaller width, the milder longitudinal slope, and the higher flow resistance of the vegetated areas in the scenarios with vegetation present (Figure 6d). The width-to-depth ratio increases with time in all scenarios, but was largest for the nonvegetated case (Scenario 1), while the vegetated cases exhibited smaller values that converged over time (Figure 6c).

Temporal variations of channel width, depth, and thus of the width-to-depth ratio are the smallest in Scenario 3, producing the most stable channel configuration, in which local bank accretion due to vegetation establishment is almost counterbalanced by erosion on the opposing side of the channel due to vegetation push. The slope of the channels increases after each high discharge episode and reduces during the low-flow periods (Figure 6d). It is particularly noticeable that the lowest values of channel slope correspond to

Table 1
Reach-Averaged Channel and Bar Characteristics at the Time of the Initial Vegetation Placement (After 31 hr)

Characteristic	Units	Scenario 1	Scenario 2	Scenario 3
Wetted channel width (B)	m	1.54	1.49	1.60
Water depth (h)	m	0.041	0.049	0.054
Slope[a] (i)	%	0.12	0.11	0.11
Mean flow velocity (u)	m/s	0.35	0.30	0.25
Maximum flow velocity (u_{Max})	m/s	0.62	0.43	0.36
Chézy coefficient (C)	$m^{1/2}/s$	49.9	40.9	32.4
Sinuosity[b] (I_S)	—	1.011	1.012	1.012
Mean shields parameter (D_{16})[c] (θ_{16})	—	0.093	0.102	0.113
Mean shields parameter (D_{50})[c] (θ_{50})	—	0.030	0.033	0.036
Mean shields parameter (D_{84})[c] (θ_{84})	—	0.021	0.023	0.026
Maximum shields parameter (D_{16})[c] (θmax_{16})	—	0.292	0.209	0.234
Maximum shields parameter (D_{50})[c] (θmax_{50})	—	0.094	0.067	0.075
Maximum shields parameter (D_{84})[c] (θmax_{84})	—	0.067	0.048	0.053
Bar length[d]	m	7.3	7.0	7.7
Bar amplitude[e]	m	0.045	0.043	0.044
Theoretical bar mode[f] (m)	—	0–1	0–1	1
Observed bar mode (m)	—	1	1	1
Sediment transport rate[g] (Q_s)	kg/hr	0.40	—	—

Note. Hydraulic variables refer to the low-flow discharge of 22 L/s.
[a]Calculated along the thalweg. [b]I_S = thalweg length divided by reach length. [c]Calculated with equation (4). Mean and maximum flow velocities are used accordingly. [d]Measured between emergent bar tops. [e]Difference in elevation between the highest and lowest locations on a bar. [f]Computed assuming $b = 4$ and $b = 10$ in equation (1). [g]Only measured for Scenario 1 during the bar formation stage.

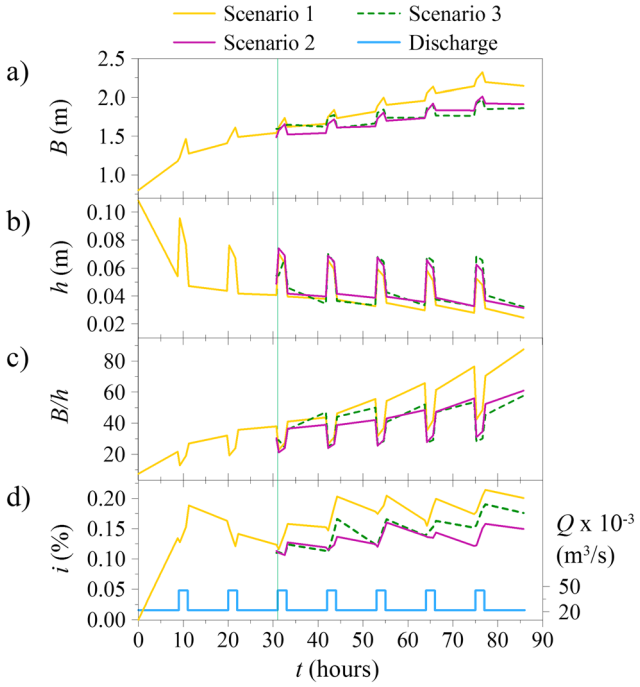

Figure 6. Temporal evolution of reach averaged: (a) wetted channel width, *B*, (b) water depth, *h*, (c) wet channel width-to-depth ratio, *B*/*h*, and (d) channel slope, *i*, during the experiments. Discharge variation, *Q*, is shown in panel (d).

Scenario 2 (vegetated floodplains), while the unvegetated case exhibits the highest slopes. Scenario 2 results in the highest sinuosity (Table 2), which can explain why this scenario presents the lowest slope.

Regarding the final configuration of each channel, Figure 7 shows the high-flow water depths, whereas Table 2 lists the main characteristics of the channels and their bars at the end of each scenario at low flow conditions. From the planview presented in Figure 7, it can be seen that three main (relatively wide) bars formed in the unvegetated case, whereas four (narrower and shorter) bars formed in the scenarios with vegetation. By analyzing the values provided in Table 2, we can observe that higher bars and deeper channels are obtained in the scenario with vegetation establishment on emerging bars (Scenario 3): the bar amplitude increases from 0.057–0.058 m in Scenarios 1 and 2, respectively, to 0.075 m in Scenario 3. This phenomenon occurs due to local sediment deposition on bar tops during high-flow conditions, enhanced by vegetation. Compared to the unvegetated case, bank erosion is substantially reduced in Scenarios 2 and 3 due to the lower erodibility of the banks, which is reflected in a reduction of average channel width. However, local bank erosion peaks are found in Scenario 3 opposite vegetated bars. This is attributed here to bank push exerted by vegetation on bar tops, resulting in flow concentration near the eroding bank and in a relatively high sediment transport rate. At the same time, Scenario 3 also presents some local channel narrowing due to the established vegetation, which results in an averaged width that is slightly smaller than that of Scenario 2. Results of Scenario 2 showed that vegetation on floodplains strongly decreased the bar wavelength with respect to the unvegetated scenario, that is, 7.5 versus 14 m. However, a bar wavelength of 10 m is observed in Scenario 3 due to extra sediment deposition upstream and downstream of vegetated bar tops.

Sediment output measurements show that more sediment was leaving the system at the end of Scenario 3, attributed here to reach-scale channel incision and flow concentration (Figure 8). This behavior is reflected

Table 2
Reach-Averaged Channel and Bar Characteristics for the Considered Scenarios After 86 hr

Characteristic	Units	Scenario 1	Scenario 2	Scenario 3
Wetted channel width (B)	m	2.15	1.91	1.86
Water depth (h)	m	0.024	0.031	0.032
Slope[a] (i)	%	0.2	0.15	0.18
Mean flow velocity (u)	m/s	0.42	0.37	0.37
Maximum flow velocity (u_{Max})	m/s	0.6	0.5	0.52
Chézy coefficient (C)	$m^{1/2}/s$	60.6	54.3	48.3
Sinuosity[b] (I_S)	—	1.028	1.042	1.039
Mean shields parameter (D_{16})[c] (θ_{16})	—	0.091	0.088	0.111
Mean shields parameter (D_{50})[c] (θ_{50})	—	0.029	0.028	0.036
Mean shields parameter (D_{84})[c] (θ_{84})	—	0.021	0.020	0.025
Maximum shields parameter (D_{16})[c] (θmax_{16})	—	0.186	0.160	0.220
Maximum shields parameter (D_{50})[c] (θmax_{50})	—	0.059	0.051	0.070
Maximum shields parameter (D_{84})[c] (θmax_{84})	—	0.042	0.037	0.050
Bar length[d]	m	14	7.5	10
Bar amplitude[e]	m	0.057	0.058	0.075
Theoretical bar mode[f] (m)	—	1–2	1–2	1–2
Observed bar mode (m)	—	1–2	1–2	1–2
Sediment transport rate (Q_s)	kg/hr	0.39	0.3	0.42

Note. Hydraulic variables refer to the low-flow discharge of 22 L/s.
[a]Calculated along the thalweg. [b]I_S = thalweg length divided by reach length. [c]Calculated with equation (4). Mean and maximum flow velocities are used accordingly. [d]Measured between emergent bar tops. [e]Difference in elevation between the highest and lowest locations on a bar. [f]Computed assuming $b = 4$ and $b = 10$ in equation (1).

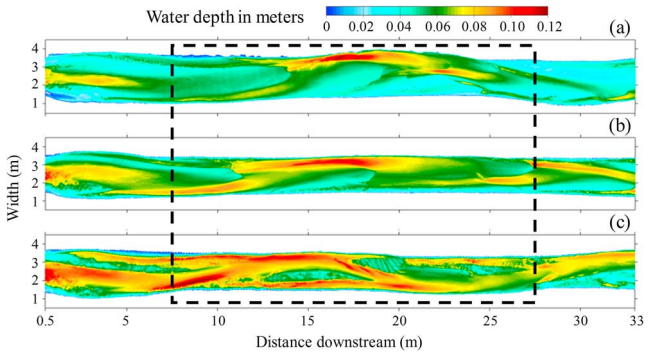

Figure 7. Measured water depths of the channel at high flow conditions after 86 hr for (a) Scenario 1, (b) Scenario 2, and (c) Scenario 3. The dashed square indicates the area used to report the reach-averaged characteristics of the channel. Flow from left to right.

in the higher water depth obtained for Scenario 3 with respect to the other two scenarios. The channel slope was higher in Scenario 1 and slightly smaller in Scenario 2 in comparison to the results obtained for Scenario 3. Another source of extra sediment identified in our experiments was given by local bank erosion. Figure 8 shows bursts of sediment transport during high flows but also during low flows. We attribute the latter to the bank failure events that occurred during the low-flow stages.

The final planforms of the channels obtained at the end of the experiments are presented in Figure 9. In this figure it is possible to observe the channel width reduction and the changes in bar pattern for the vegetated scenarios (i.e., a higher number of bars and wavelength reduction). The thalweg line for each scenario is shown with a dashed yellow line. Thalweg lines demonstrate the higher sinuosity obtained for the cases with added vegetation and emphasize that the case with vegetated floodplains (Scenario 2) exhibits the higher sinuosity for this investigation. Small back-bar channels are indicated by the points marked as number 1 in Figure 9c, while number 2 shows that the bar top is higher near the channel centerline, as indicated by the presence of vegetation.

4. Discussion

Our results agree with the numerical findings of Bywater-Reyes et al. (2018) and the experimental observations of Rominger et al. (2010) in a curved channel with fixed banks, who found that vegetation establishment on a bar directs the flow toward the opposite bank. At the same time, they found that the establishment of vegetation increases the rates of bar accretion through velocity reduction upstream and downstream of vegetated areas, which coincides with our measurements.

Jang and Shimizu (2005) simulated the response of migrating bars to the establishment of riparian vegetation by increasing the bank strength in a numerical model through variation of the critical angle of repose of the bank material. Their results show that higher bank strength produced narrower channels and thus smaller width-to-depth ratios, smaller bar amplitudes, and faster bar migration rates, as well as shorter bar wavelengths in the channel. This morphological response was explained theoretically by Tubino and Seminara (1990), who showed that the larger the channel width-to-depth ratio is, the longer bars are and the slower their movement. The bar dynamics described in the above studies agree with our observations and the planforms obtained at the end of the experiments (Figure 9).

Our experimental results are also supported by field observations. Erskine et al. (2012) show channel narrowing as a response to vegetation growth on floodplains and bars from the temporal changes of the Widden Brook (Australia). Loozen (2017) analyzed the morphodynamic processes of the Colorado River (Arizona) with a numerical model to explain why sandbars tend to stabilize the soil, causing the channel to become narrower after bar and floodplain colonization by plants (Birkeland, 1996). Stabilization and elongation of gravel bars after vegetation establishment were also observed in the Isère River (France) by Serlet et al. (2018). Other real-case examples are reported by Gurnell (2014), who also describes how vegetation growth increases the size of pioneer islands in the Tagliamento River (Italy).

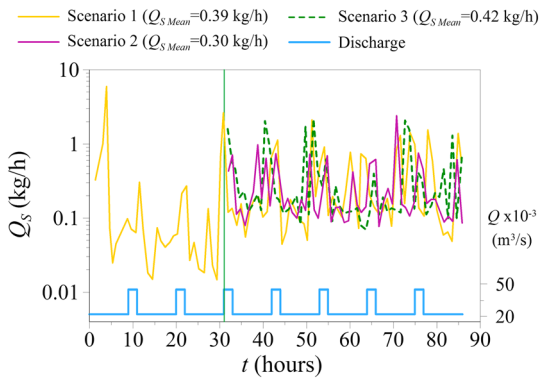

Figure 8. Temporal evolution of sediment output (Q_S). The values shown in the legend correspond to the average for each scenario calculated for the period between 31 and 86 hr. The discharge, Q, is shown for reference.

The highest areas of the bars in our experiments were not attached to the floodplain but were located toward the center of the channel. During their evolution from the initial flat bed, bars first formed attached to the banks (alternate bars). Simultaneous channel widening, caused by progressive bank erosion, increased the width-to-depth ratio of the flow, increasing the bar mode as well. As a result, alternate bars tended to become central bars, which led to the formation of sediment deposits, increasing the alternate bar elevation near the center of the channel. This resulted in the

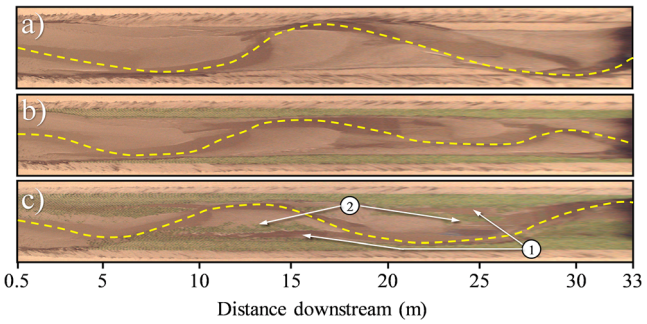

Figure 9. Planview photographs of the channels after 86 hr for (a) Scenario 1, (b) Scenario 2, and (c) Scenario 3. Small, back bar channels are indicated by the points marked as number 1, while number 2 shows that the bar top is higher near the channel centerline, as indicated by the presence of vegetation. The dashed yellow line corresponds to the thalweg for each scenario. Flow from left to right.

gradual development of an anabranched system, with a small channel forming between the vegetated areas of bars and the bank to which bars were initially attached (i.e., the formation of the back-bar channels or chutes; Figures 7 and 9). The absence of fine suspended sediments, floating vegetation, and organic matter in our experiments that might otherwise block and fill in these smaller channels also contributes to the formation of the incipient anabranched system. However, the flow convergence and divergence zones and the combination of small channels with varied hierarchy described by Church (1992) demonstrate that the existence of these "back-bar channels" is common in gravel-bed streams. The observations and analyses of Tooth and Nanson (2000) and Huang and Nanson (2007), who highlight the role of vegetation establishment on bars in channel anabranching, support our findings on the effects of vegetation colonization in this process. The observed and theoretical bar modes at the end of each scenario (Table 2) indeed show that the type of bars present in the system fell between alternate and central bars (Modes 1 and 2).

After the first 31 hr, none of the scenarios showed increasing or decreasing trends in sediment transport rate, indicating the establishment of morphodynamic equilibrium. Reach-scale equilibrium, however, also requires negligible changes in longitudinal channel slope. Figure 6 shows that in Scenarios 1 and 3 the slope reached a dynamic equilibrium after about 55 hr, notwithstanding the evolution trends of water depth and wetted channel width. The slight increasing trend of longitudinal slope shows that Scenario 2 did not fully attain a state of reach-scale equilibrium at the end of the experiment. This can be explained by the sediment transport rates (Table 2). Sediment transport was the smallest in Scenario 2, which increases the duration of morphological adaptation compared to the other two scenarios.

Based on sediment mobility (determined by calculating the Shields parameter, equation (4)), we find that the experimental channels exhibit mobility values similar to gravel-bed rivers, characterized by conditions close to initiation of motion (assuming 0.030 as the threshold for sediment mobility) for the majority of the time (e.g., Adami et al., 2016). In the experiments, only the smallest sediment fractions are always mobile (Tables 1 and 2). At low flows, the largest grain sizes move only in the deeper portions of the channel where the flow concentrates and the maximum velocities are found, whereas they are left behind in areas with low-flow velocity.

The interpretation of our experimental results at the scale of natural rivers is particularly complicated because of the difficulty of upscaling vegetation. It is not possible to determine which type of floodplain vegetation is represented by the plastic plants that were used in the experiments. This is not due to the use of artificial vegetation, because the scaling issue also would be similar if we had employed real plants as, for instance, was done by Tal and Paola (2007, 2010). As such, application of our findings to natural systems remains imperfect, and although our observations highlight important aspects of the interaction between vegetation and the flow of water and sediment, they cannot be directly extrapolated to a specific river system. In addition to the latter, the experiments describe systems in which the discharge did not easily eradicate plants during high flow stages. Resistance to high-flow uprooting is observed in small streams, like the Lunterse beek in the Netherlands (Vargas-Luna et al., 2019). However, the experiments cannot be considered representative of large river systems, where plants have a less dominant role. This relative effect of vegetation depending on the size of the river is consistent with previous observations in other large-scale experiments (e.g., Bertagni et al., 2018) and by means of numerical modeling (e.g., Kui et al., 2014).

5. Conclusions

To visualize and quantify the morphological effects of vegetation establishment on emergent bar tops, we carried out a series of laboratory experiments. These were carried out in a mobile bed, large-scale, laboratory stream table with sediment recirculation and variable discharge. We compared the morphological evolution of the following three scenarios, starting from unvegetated channels with alternate bars: (1) channel without vegetation, (2) channel with vegetation establishment on floodplains, and (3) channel with vegetation establishment on floodplains and bar tops during low-flow stages.

The results show that vegetation establishment on floodplains reduces bank erosion and that vegetation establishment on bar tops increases bar amplitude and deflects the flow toward the opposite side of the channel (bank push), increasing local bank erosion. Vegetation establishment strongly modifies the bar properties and the planform configuration of alluvial channels. By decreasing the bank erosion rates and the width-to-depth ratio, floodplain vegetation results in reduced alternate bar lengths with respect to the unvegetated case (46.4% and 28.6% lower for Scenarios 2 and 3, respectively). If vegetation also establishes itself on bar tops, local sediment supply is trapped, producing bar elongation. This means that the final bar morphology observed in alluvial rivers is caused by the flow regime and sediment characteristics of the system and the relative effects of the colonizing vegetation on bars and river floodplains.

The scenario with vegetation establishment on floodplains and emerging bar tops produces a more stable morphology over time. Although the channel continues to be dynamic, local bank accretion and erosion of the opposing bank seem to almost counterbalance each other. This is the typical behavior of meandering rivers. These rivers are indeed mostly found in areas with relatively fast vegetation growth, in tropical and humid climates (Ebisemiju, 1994).

Our experimental observations indicate that the major effect of vegetation establishment on bar tops during low-flow periods is bar accretion and an increase in localized bank erosion. This would enhance river meandering or anabranching depending on channel width-to-depth ratio, which in turn depends on bank erodibility: low width-to-depth ratios resulting in alternate bar formation would lead to river meandering (relatively low bank erodibility), whereas larger width-to-depth ratios resulting in central (or multiple) bar formation would lead to river anabranching (relatively high bank erodibility). Compared to the case in which vegetation establishes itself on river floodplains only, in our experiments the channel width is only slightly affected by the presence of vegetation on bar tops.

Acknowledgments
Andrés Vargas-Luna is grateful to COLCIENCIAS (Colombian Administrative Department of Science, Technology and Innovation, Grant 512 of 2010) and to Pontificia Universidad Javeriana, the two institutions that financially supported his studies in the Netherlands. The authors express their gratitude to the personnel of the Environmental Fluid Mechanics Laboratory of Delft University of Technology for the collaboration during the execution of the experiments. This research has also benefited from cooperation within the network of the Netherlands Center for River studies. The authors also thank the reviewers and Editors for their thorough and thoughtful review. The obtained experimental data are freely available online (https://doi.org/10.6084/m9.figshare.7591643).

References

Abernethy, B., & Rutherfurd, I. D. (2000). Does the weight of riparian trees destabilize riverbanks? *Regulated Rivers: Research & Management*, *16*(6), 565–576. https://doi.org/10.1002/1099-1646(200011/12)16:6<565::AID-RRR585>3.0.CO;2-1

Adami, L., Bertoldi, W., & Zolezzi, G. (2016). Multidecadal dynamics of alternate bars in the alpine Rhine river. *Water Resources Research*, *52*, 8938–8955. https://doi.org/10.1002/2015WR018228

Allen, C. D., Macalady, A. K., Chenchouni, H., Bachelet, D., McDowell, N., Vennetier, M., et al. (2010). A global overview of drought and heat-induced tree mortality reveals emerging climate change risks for forests. *Forest Ecology and Management*, *259*(4), 660–684. https://doi.org/10.1016/j.foreco.2009.09.001

Allmendinger, N. E., Pizzuto, J. E., Potter, N., Johnson, T. E., & Hession, W. C. (2005). The influence of riparian vegetation on stream width, Eastern Pennsylvania, USA. *Geological Society of America Bulletin*, *117*(1), 229–243. https://doi.org/10.1130/B25447.1

Asahi, K., Shimizu, Y., Nelson, J., & Parker, G. (2013). Numerical simulation of river meandering with self-evolving banks. *Journal of Geophysical Research: Earth Surface*, *118*, 2208–2229. https://doi.org/10.1002/jgrf.20150

Asselman, N. E. M. (1995). In S. Zwerver, R. S. A. R. Rompaey, M. T. J. van Kok, & M. M. Berk (Eds.), *The impact of climate change on suspended sediment transport in the river Rhine, in Climate change research: Evaluation and policy implications; Proceedings of the International Climate Change Research Conference, Vol. B, Studies in Environmental Science*, (Vol. 65, pp. 937–942). Maastricht, The Netherlands, 6-9 December 1994: Elsevier.

Bankhead, N. L., Thomas, R. E., & Simon, A. (2017). A combined field, laboratory and numerical study of the forces applied to, and the potential for removal of, bar top vegetation in a braided river. *Earth Surface Processes and Landforms*, *42*(3), 439–459. https://doi.org/10.1002/esp.3997

Bertagni, M. B., Perona, P., & Camporeale, C. (2018). Parametric transitions between bare and vegetated states in water-driven patterns. *Proceedings of the National Academy of Sciences*, *115*(32), 8125–8130. https://doi.org/10.1073/pnas.1721765115

Bertoldi, W., Siviglia, A., Tettamanti, S., Tofolon, M., Vetsch, D., & Francalanci, S. (2014). Modeling vegetation controls on fluvial morphological trajectories. *Geophysical Research Letters*, *41*, 7167–7175. https://doi.org/10.1002/2014GL061666

Bertoldi, W., Welber, M., Gurnell, A. M., Mao, L., Comiti, F., & Tal, M. (2015). Physical modelling of the combined effect of vegetation and wood on river morphology. *Geomorphology*, *246*, 178–187. https://doi.org/10.1016/j.geomorph.2015.05.038

Birkeland, G. H. (1996). Riparian vegetation and sandbar morphology along the lower little Colorado River, Arizona. *Physical Geography*, *17*(6), 534–553. https://doi.org/10.1080/02723646.1996.10642600

Braudrick, C. A., Dietrich, W. E., Leverich, G. T., & Sklar, L. S. (2009). Experimental evidence for the conditions necessary to sustain meandering in coarse bedded rivers. *Proceedings of the National Academy of Sciences*, *106*(40), 16936–16941. https://doi.org/10.1073/pnas.0909417106

Brevis, W., Niño, Y., & Jirka, G. H. (2011). Integrating cross-correlation and relaxation algorithms for particle tracking velocimetry. *Experiments in Fluids*, *50*(1), 135–147. https://doi.org/10.1007/s00348-010-0907-z

Byishimo, P. (2014), Effects of variable discharge on width formation and cross-sectional shape of sinuous rivers, Master's thesis, UNESCO-IHE, Institute for Water Education, Delft, The Netherlands.

Bywater-Reyes, S., Diehl, R. M., & Wilcox, A. C. (2018). The influence of a vegetated bar on channel-bend flow dynamics. *Earth Surface Dynamics*, *6*(2), 487–503. https://doi.org/10.5194/esurf-6-487-2018

Bywater-Reyes, S., Wilcox, A. C., Stella, J. C., & Lightbody, A. F. (2015). Flow and scour constraints on uprooting of pioneer woody seedlings. *Water Resources Research*, *51*, 9190–9206. https://doi.org/10.1002/2014WR016641

Church, M. (1992). Channel morphology and typology. In P. Carlow, & G. E. Petts (Eds.), *The rivers handbook: Hydrological and ecological principles*, (pp. 126–143). Oxford: Blackwell Scientific Publications.

Collison, A. J. C., & Anderson, M. G. (1996). Using a combined slope hydrology/stability model to identify suitable conditions for landslide prevention by vegetation in the humid tropics. *Earth Surface Processes and Landforms*, *21*(8), 737–747. https://doi.org/10.1002/(SICI)1096-9837(199608)21:8<737::AID-ESP674>3.0.CO;2-F

Corenblit, D., Steiger, J., Gurnell, A. M., & Naiman, R. J. (2009). Plants intertwine fluvial landform dynamics with ecological succession and natural selection: a niche construction perspective for riparian systems. *Global Ecology and Biogeography*, *18*(4), 507–520. https://doi.org/10.1111/j.1466-8238.2009.00461.x

Cotton, J. A., Wharton, G., Bass, J. A. B., Heppell, C. M., & Wotton, R. S. (2006). The effects of seasonal changes to in-stream vegetation cover on patterns of flow and accumulation of sediment. *Geomorphology*, *77*(3-4), 320–334. https://doi.org/10.1016/j.geomorph.2006.01.010

Crosato, A., Desta, F. B., Cornelisse, J., Schuurman, F., & Uijttewaal, W. S. J. (2012). Experimental and numerical findings on the long-term evolution of migrating alternate bars in alluvial channels. *Water Resources Research*, *48*, W06524. https://doi.org/10.1029/2011WR011320

Crosato, A., & Mosselman, E. (2009). Simple physics-based predictor for the number of river bars and the transition between meandering and braiding. *Water Resources Research*, *45*, W03424. https://doi.org/10.1029/2008WR007242

Crosato, A., & Samir Saleh, M. (2011). Numerical study on the effects of floodplain vegetation on river planform style. *Earth Surface Processes and Landforms*, *36*(6), 711–720. https://doi.org/10.1002/esp.2088

Diehl, R. M., Wilcox, A. C., Stella, J. C., Kui, L., Sklar, L. S., & Lightbody, A. (2017). Fluvial sediment supply and pioneer woody seedlings as a control on bar surface topography. *Earth Surface Processes and Landforms*, *42*(5), 724–734. https://doi.org/10.1002/esp.4017

Duró, G., Crosato, A., & Tassi, P. (2016). Numerical study on river bar response to spatial variations of channel width. *Advances in Water Resources*, *93*, 21–38. https://doi.org/10.1016/j.advwatres.2015.10.003

Eaton, B., Millar, R. G., & Davidson, S. (2010). Channel patterns: Braided, anabranching, and single-thread. *Geomorphology*, *120*(3-4), 353–364. https://doi.org/10.1016/j.geomorph.2010.04.010

Ebisemiju, F. S. (1994). The sinuosity of alluvial river channels in the seasonally wet tropical environment: Case study of river elemi, southwestern Nigeria. *Catena*, *21*(1), 13–25. https://doi.org/10.1016/0341-8162(94)90028-0

Edmaier, K., Burlando, P., & Perona, P. (2011). Mechanisms of vegetation uprooting by ow in alluvial non-cohesive sediment. *Hydrology and Earth System Sciences Discussions*, *8*(1), 1365–1398. https://doi.org/10.5194/hessd-8-1365-2011

Edmaier, K., Crouzy, B., & Perona, P. (2015). Experimental characterization of vegetation uprooting by flow. *Journal of Geophysical Research: Biogeosciences*, *120*, 1812–1824. https://doi.org/10.1002/2014JG002898

Egger, G., Politti, E., Lautsch, E., Benjankar, R., Gill, K. M., & Rood, S. B. (2015). Floodplain forest succession reveals fluvial processes: A hydrogeomorphic model for temperate riparian woodlands. *Journal of Environmental Management*, *161*, 72–82. https://doi.org/10.1016/j.jenvman.2015.06.018

El Kadi Abderrazzak, K., Die Moran, A., Mosselman, E., Bouchard, J.-P., Habersack, H., & Aelbrecht, D. (2014). A physical, movable-bed model for non-uniform sediment transport, fluvial erosion and bank failure in rivers. *Journal of Hydro-environment Research*, *8*(2), 95–114. https://doi.org/10.1016/j.jher.2013.09.004

Engelund, F. (1970). Instability of erodible beds. *Journal of Fluid Mechanics*, *42*(3), 225–244. https://doi.org/10.1017/S0022112070001210

Erskine, W., A. Keene, R. Bush, M. Cheetham, and A. Chalmers (2012), Influence of riparian vegetation on channel widening and subsequent contraction on a sand-bed stream since European settlement: Widden brook, Australia, Geomorphology, 147-148, 102-114, doi:10.1016/j.geomorph.2011.07.030, geomorphology of Large Rivers - cases from the 7th (IAG) Conference, Melbourne.

Folkard, A. M. (2011). Vegetated flows in their environmental context: A review, Proceedings of the Institution of Civil Engineers. *Engineering and Computational Mechanics*, *164*(1), 3–24. https://doi.org/10.1680/eacm.8.00006

Gleason, C. J. (2015). Hydraulic geometry of natural rivers: A review and future directions. *Progress in Physical Geography*, *39*(3), 337–360. https://doi.org/10.1177/0309133314567584

Gran, K., & Paola, C. (2001). Riparian vegetation controls on braided stream dynamics. *Water Resources Research*, *37*(12), 3275–3283. https://doi.org/10.1029/2000WR000203

Gran, K. B., Tal, M., & Wartman, E. D. (2015). Co-evolution of riparian vegetation and channel dynamics in an aggrading braided river system, mount Pinatubo, Philippines. *Earth Surface Processes and Landforms*, *40*(8), 1101–1115. https://doi.org/10.1002/esp.3699

Green, J. C. (2005). Modelling flow resistance in vegetated streams: Review and development of new theory. *Hydrological Processes*, *19*(6), 1245–1259. https://doi.org/10.1002/hyp.5564

Gurnell, A. M. (2014). Plants as river system engineers. *Earth Surface Processes and Landforms*, *39*(1), 4–25. https://doi.org/10.1002/esp.3397

Gurnell, A. M., Bertoldi, W., & Corenblit, D. (2012). Changing river channels: The roles of hydrological processes, plants and pioneer fluvial landforms in humid temperate, mixed load, gravel bed rivers. *Earth-Science Reviews*, *111*(1-2), 129–141. https://doi.org/10.1016/j.earscirev.2011.11.005

Hickin, E. J. (1984). Vegetation and river channel dynamics. *Canadian Geographer/Le Géographe Canadien*, *28*(2), 111–126. https://doi.org/10.1111/j.1541-0064.1984.tb00779.x

Huang, H. Q., & Nanson, G. C. (2007). Why some alluvial rivers develop an anabranching pattern. *Water Resources Research*, *43*, W07441. https://doi.org/10.1029/2006WR005223

Iwasaki, T., Shimizu, Y., & Kimura, I. (2016). Numerical simulation of bar and bank erosion in a vegetated floodplain: A case study in the Otofuke River. *Advances in water resources*, *93*, 118–134. https://doi.org/10.1016/j.advwatres.2015.02.001

Jang, C., & Shimizu, Y. (2007). Vegetation effects on the morphological behavior of alluvial channels. *Journal of Hydraulic Research*, *45*(6), 763–772. https://doi.org/10.1080/00221686.2007.9521814

Jang, C.-L., & Shimizu, Y. (2005). Numerical simulations of the behavior of alternate bars with different bank strengths. *Journal of Hydraulic Research*, *43*(6), 596–612. https://doi.org/10.1080/00221680509500380

Jones, C. G., Lawton, J. H., & Shachak, M. (1994). Organisms as ecosystem engineers. *Oikos*, *69*(3), 373–386. https://doi.org/10.2307/3545850

Kang, T., Kimura, I., & Shimizu, Y. (2018). Responses of bed morphology to vegetation growth and flood discharge at a sharp river bend. *Water*, *10*(2), 1–25. https://doi.org/10.3390/w10020223

Kleinhans, M. G., van Dijk, W. M., van de Lageweg, W. I., Hoyal, D. C. J. D., Markies, H., van Maarseveen, M., et al. (2014). Quantifiable effectiveness of experimental scaling of river- and delta morphodynamics and stratigraphy. *Earth-Science Reviews*, *133*, 43–61. https://doi.org/10.1016/j.earscirev.2014.03.001

van de Koppel, J., Herman, P. M. J., Thoolen, P., & Heip, C. H. R. (2001). Do alternate stable states occur in natural ecosystems? Evidence from a tidal flat. *Ecology*, *82*(12), 3449–3461. https://doi.org/10.1890/0012-9658(2001)082[3449:DASSOI]2.0.CO;2

Kui, L., Stella, J. C., Lightbody, A., & Wilcox, A. C. (2014). Ecogeomorphic feedbacks and flood loss of riparian tree seedlings in meandering channel experiments. *Water Resources Research*, *50*, 9366–9384. https://doi.org/10.1002/2014WR015719

Le, T. B., Crosato, A., & Uijttewaal, W. S. J. (2018). Long-term morphological developments of river channels separated by a longitudinal training wall. *Advances in Water Resources*, *113*, 73–85. https://doi.org/10.1016/j.advwatres.2018.01.007

Loozen, M. M. (2017), Relation between riparian vegetation and sandbar dynamics in the Colorado River, Master's thesis, Delft University of Technology, Delft, The Netherlands.

Lotsari, E., Thorndycraft, V., & Alho, P. (2015). Prospects and challenges of simulating river channel response to future climate change. *Progress in Physical Geography: Earth and Environment*, *39*(4), 483–513. https://doi.org/10.1177/0309133315578944

Marjoribanks, T. I., Hardy, R. J., & Lane, S. N. (2014). The hydraulic description of vegetated river channels: The weaknesses of existing formulations and emerging alternatives. *WIREs Water*, *1*(6), 549–560. https://doi.org/10.1002/wat2.1044

Meier, C. I., Reid, B. L., & Sandoval, O. (2013). Effects of the invasive plant Lupinus Polyphyllus on vertical accretion of fine sediment and nutrient availability in bars of the gravel-bed Paloma river. *Limnologica - Ecology and Management of Inland Waters*, *43*(5), 381–387. https://doi.org/10.1016/j.limno.2013.05.004

Millar, R. G. (2000). Influence of bank vegetation on alluvial channel patterns. *Water Resources Research*, *36*(4), 1109–1118. https://doi.org/10.1029/1999WR900346

Millar, R. G. (2005). Theoretical regime equations for mobile gravel-bed rivers with stable banks. *Geomorphology*, *64*(3-4), 207–220. https://doi.org/10.1016/j.geomorph.2004.07.001

Mueller, E., & Pitlick, J. (2013). Sediment supply and channel morphology in mountain river systems: 1. Relative importance of lithology, topography, and climate. *Journal of Geophysical Research: Earth Surface*, *118*, 2325–2342. https://doi.org/10.1002/2013JF002843

Murray, A. B., & Paola, C. (2003). Modelling the effect of vegetation on channel pattern in bedload rivers. *Earth Surface Processes and Landforms*, *28*(2), 131–143. https://doi.org/10.1002/esp.428

Nepf, H. M. (2012). Flow and transport in regions with aquatic vegetation. *Annual Review of Fluid Mechanics*, *44*(1), 123–142. https://doi.org/10.1146/annurev-uid-120710-101048

Nikora, V. (2010). Hydrodynamics of aquatic ecosystems: An interface between ecology, biomechanics and environmental fluid mechanics. *River Research and Applications*, *26*(4), 367–384. https://doi.org/10.1002/rra.1291

Paola, C. (2011). Co-evolution of rivers and plants. *Nature Geoscience*, *4*(9), 583–584. https://doi.org/10.1038/ngeo1247

Perona, P., & Crouzy, B. (2018). Resilience of riverbed vegetation to uprooting by flow, Proceedings of the Royal Society of London A: Mathematical. *Physical and Engineering Sciences*, *474*(2211). https://doi.org/10.1098/rspa.2017.0547

Perry, L. G., Reynolds, L. V., Beechie, T. J., Collins, M. J., & Shafroth, P. B. (2015). Incorporating climate change projections into riparian restoration planning and design. *Ecohydrology*, *8*(5), 863–879. https://doi.org/10.1002/eco.1645

Perucca, E., Camporeale, C., & Ridolfi, L. (2007). Significance of the riparian vegetation dynamics on meandering river morphodynamics. *Water Resources Research*, *43*, W03430. https://doi.org/10.1029/2006WR005234

Pollen, N., & Simon, A. (2005). Estimating the mechanical effects of riparian vegetation on stream bank stability using a fiber bundle model. *Water Resources Research*, *41*, W07025. https://doi.org/10.1029/2004WR003801

Pollen-Bankhead, N., & Simon, A. (2010). Hydrologic and hydraulic effects of riparian root networks on streambank stability: Is mechanical root-reinforcement the whole story? *Geomorphology*, *116*(3-4), 353–362. https://doi.org/10.1016/j.geomorph.2009.11.013

Polvi, L. E., Wohl, E., & Merritt, D. M. (2014). Modeling the functional influence of vegetation type on streambank cohesion. *Earth Surface Processes and Landforms*, *39*(9), 1245–1258. https://doi.org/10.1002/esp.3577

Rominger, J. T., Lightbody, A. F., & Nepf, H. M. (2010). Effects of added vegetation on sand bar stability and stream hydrodynamics. *Journal of Hydraulic Engineering*, *136*(12), 994–1002. https://doi.org/10.1061/(ASCE)HY.1943-7900.0000215

van Ruijven, J., & Berendse, F. (2005). Diversity-productivity relationships: Initial effects, long-term patterns, and underlying mechanisms. *Proceedings of the National Academy of Sciences of the United States of America*, *102*(3), 695–700. https://doi.org/10.1073/pnas.0407524102

Sand-Jensen, K., & Mebus, J. R. (1996). Fine-scale patterns of water velocity within macrophyte patches in streams. *Oikos*, *76*(1), 169–180. https://doi.org/10.2307/3545759

Serlet, A. J., Gurnell, A. M., Zolezzi, G., Wharton, G., Belleudy, P., & Jourdain, C. (2018). Biomorphodynamics of alternate bars in a channelized, regulated river: An integrated historical and modelling analysis. *Earth Surface Processes and Landforms*, *43*(9), 1739–1756. https://doi.org/10.1002/esp.4349

Shields, A. (1936). Anwendung der Aehnlichkeitsmechanik und der Turbulenzforschung auf die Geschiebebewegung. PhD Thesis Technical University Berlin.

Simon, A., & Collison, A. J. C. (2002). Quantifying the mechanical and hydrologic effects of riparian vegetation on streambank stability. *Earth Surface Processes and Landforms*, *27*(5), 527–546. https://doi.org/10.1002/esp.325

Struiksma, N., Olesen, K. W., Flokstra, C., & De Vriend, H. J. (1985). Bed deformation in curved alluvial channels. *Journal of Hydraulic Research*, *23*(1), 57–79. https://doi.org/10.1080/00221688509499377

Tal, M., & Paola, C. (2007). Dynamic single-thread channels maintained by the interaction of ow and vegetation. *Geology*, *35*(4), 347–350. https://doi.org/10.1130/G23260A.1

Tal, M., & Paola, C. (2010). Effects of vegetation on channel morphodynamics: Results and insights from laboratory experiments. *Earth Surface Processes and Landforms*, *35*(9), 1014–1028. https://doi.org/10.1002/esp.1908

Terwilliger, V. J. (1990). Effects of vegetation on soil slippage by pore pressure modification. *Earth Surface Processes and Landforms*, *15*(6), 553–570. https://doi.org/10.1002/esp.3290150607

Tooth, S., & Nanson, G. C. (2000). The role of vegetation in the formation of anabranching channels in an ephemeral river, northern plains, arid central Australia. *Hydrological Processes*, *14*(16-17), 3099–3117. https://doi.org/10.1002/1099-1085(200011/12)14:16/17<3099::AID-HYP136>3.0.CO;2-4

Tsujimoto, T. (1999). Fluvial processes in streams with vegetation. *Journal of Hydraulic Research*, *37*(6), 789–803. https://doi.org/10.1080/00221689909498512

Tubino, M., & Seminara, G. (1990). Free-forced interactions in developing meanders and suppression of free bars. *Journal of Fluid Mechanics*, *214*(1), 131–159. https://doi.org/10.1017/S0022112090000088

Van Rijn L.C. (1993). Principles of sediment transport in rivers, estuaries and coastal seas. Part I: Edition 1993. Aqua Publications, the Netherlands, www.aquapublications.nl

Vargas-Luna, A. (2016), Role of vegetation on river-bank accretion, Ph.D. thesis, Delft University of Technology, Delft, The Netherlands.

Vargas-Luna, A., Crosato, A., Anders, N., Hoitink, A. J., Keesstra, S. D., & Uijttewaal, W. S. (2018). Morphodynamic effects of riparian vegetation growth after stream restoration. *Earth Surface Processes and Landforms*, *43*(8), 1591–1607. https://doi.org/10.1002/esp.4338

Vargas-Luna, A., Crosato, A., Byishimo, P., & Uijttewaal, W. S. J. (2019). Impact of flow variability and sediment characteristics on channel width evolution in laboratory streams. *Journal of Hydraulic Research*, *57*(1), 51–61. https://doi.org/10.1080/00221686.2018.1434836

Vargas-Luna, A., Crosato, A., Calvani, G., & Uijttewaal, W. S. J. (2016). Representing plants as rigid cylinders in experiments and models. *Advances in Water Resources*, *93*, 205–222. https://doi.org/10.1016/j.advwatres.2015.10.004

Vargas-Luna, A., Crosato, A., Collot, L., and Uijttewaal, W. S. J. (2015), Laboratory investigation on the hydrodynamic characterization of artificial grass, in E-proceedings of the 36th IAHR World Congress 28 June-3 July, 2015, The Hague, the Netherlands. ISBN: 978-90-824846-0-1., pp. 728-734.

Vargas-Luna, A., Crosato, A., & Uijttewaal, W. S. J. (2015). Effects of vegetation on flow and sediment transport: Comparative analyses and validation of predicting models. *Earth Surface Processes and Landforms*, *40*(2), 157–176. https://doi.org/10.1002/esp.3633

Wintenberger, C. L., Rodrigues, S., Bréhéret, J.-G., & Villar, M. (2015). Fluvial islands: First stage of development from nonmigrating (forced) bars and woody-vegetation interactions. *Geomorphology*, *246*, 305–320. https://doi.org/10.1016/j.geomorph.2015.06.026

Wu, W., & He, Z. (2009). Effects of vegetation on flow conveyance and sediment transport capacity. *International Journal of Sediment Research*, *24*(3), 247–259. https://doi.org/10.1016/S1001-6279(10)60001-7

Zong, L., & Nepf, H. (2011). Spatial distribution of deposition within a patch of vegetation. *Water Resources Research*, *47*, W03516. https://doi.org/10.1029/2010WR009516